Physicochem. Probl. Miner. Process., 59(3), 2023, 170899

http://www.journalssystem.com/ppmp

Physicochemical Problems of Mineral Processing

ISSN 1643-1049

A nanoparticle cationic polystyrene-co-poly(n-butylacrylate) collector to eliminate the negative effect of lizardite slimes in pyrite flotation

Guanghua Ai [1], Cheng Liu [2,3], Guangli Zhu [4], Siyuan Yang [2,3]

[1] School of Resource and Environment Engineering, Jiangxi University of Science and Technology, Ganzhou 34100, China

[2] School of Resources and Environmental Engineering, Wuhan University of Technology, Wuhan, 430070, China

[3] Key Laboratory of Green Utilization of Critical Non-metallic Mineral Resources of Ministry of Education, Wuhan, Hubei 430070, China

[4] Zhongyuan Critical Metals Laboratory, Zhengzhou University, Zhengzhou, 450001, China

Corresponding author: liucheng309@whut.edu.cn (Cheng Liu), guanglizhu@zzu.edu.cn (Guangli Zhu)

Abstract: Lizardite slime coating is one of significant factors in the deterioration of the floatability of sulphide minerals. In this study, a nanoparticle cationic polystyrene-co-poly(n-butylacrylate)(PS-PBNH) collector was introduced to eliminate the negative impact of lizardite slimes in pyrite flotation. Microflotation results demonstrated that lizardite slims did not affect the recovery of pyrite in the presence of PS-PBNH. Good flotation separation of pyrite from lizardite was achieved when the nanoparticle PS-PBNH collector was used. The results from adsorption study indicated that PS-PBNH exhibited a significant adsorption on the pyrite surface in the presence of lizardite slimes. Sedimentation tests showed that hetero-aggregation occurred between lizardite slimes and pyrite, whereas the introduction of PS-PBNH collector resulted in a heterogeneous dispersion between them. Zeta potential measurements suggested that PS-PBNH collector interacted with pyrite surface, and the PS-PBNH adsorption changed the surface charge of pyrite from negative to be positive. As a result, the interaction of pyrite with lizardite shifted from electrostatic attraction to electrostatic repulsion, as supported by the DLVO calculations. These results indicated PS-PBNH can be used as a potential collector for pyrite flotation in pyrite/lizardite slimes system without the need for a depressant.

Keywords: nanoparticle collector, pyrite, lizardite slimes, flotation separation

1. Introduction

Lizardite is a phyllosilicate mineral containing magnesium and belongs to the serpentine family. Its chemical formula is $Mg_3Si_2O_5(OH)_4$ (Adebayo et al., 2013; Evans et al., 2013; Sirota et al., 2018; O'Hanley 1996). The structural unit of lizardite consists of one layer of Mg-O tetrahedral and one layer of Si-O tetrahedral. However, the Mg-O tetrahedral layer is 3%~5% larger in space than the Si-O tetrahedral layer (Wicks and Whittaker, 1975). Within this structure, magnesium ions are commonly substituted by aluminium, nickel, iron, and manganese ions (Bailey, 1988; Frost et al., 2013). In natural, lizardite is associated with fluid migration and metasomatism during serpentinization of ultrabasic rocks, which commonly occurred in sulfide deposits, particularly in nickel ores (Deng et al., 2020; Liu et al., 2018). Therefore, lizardite is a common gangue mineral for sulfide minerals. The contents of these valuable sulfide minerals in these ores are usually insufficient for direct smelting. Therefore, these ores need to undergo beneficiation to recover the valuable sulfide minerals.

At present, flotation method is usually used for the separation of sulfide minerals from magnesium silicate minerals, with xanthates as collectors (Liu et al., 2018a and 2018b; Liu et al., 2021; Yang et al., 2020; Tang and Chen, 2022; Yang et al., 2022). However, during the grinding process, lizardite tends to form slimes due to its low Mohs hardness (Liu et al., 2018b; Feng et al., 2018). Unfortunately, these hydrophilic lizardite slimes easily coat the surface of sulfide minerals due to the opposite surface charge between these two mineral types Consequently, this coating reduces the collector adsorption on sulfide mineral surface, thereby decreasing its floatability (Yu et al., 2019). To eliminate the negative influence

DOI: 10.37190/ppmp/170899

of lizardite slimes in sulfide mineral flotation, various inhibitors have been studied, including water glass (Feng et al., 2012), carboxymethylcellulose, and sodium carbonate (Feng and Luo, 2013, Zhang et al., 2017). However, these depressants still have many limitations in flotation, such as low solubility, low selectively, and high consumption (economic pressure), Therefore, the removal of lizardite slimes in sulfide mineral flotation remains a challenge task.

Currently, in the flotation separation of pyrite from lizardite, xanthates are the commonly used collectors. However, the slime coatings hinder the adsorption of these collectors onto the pyrite surface in the absence of depressants (Liu et al., 2018; Liu et al., 2021). Therefore, in the absence of depressants, achieving effective separation between pyrite and lizardite slimes becomes challenging. In the early stages of our research, we made an intriguing discovery that the nanoparticle collectors could be used for pentlandite ores separation as well as other minerals separation (Yang et al., 2011; Yang and Felton, 2011; Yang et al., 2013; Dong et al., 2016; Yang et al., 2012). This finding potentially provided a novel approach for sulfide minerals/lizardite slimes separation.

One such promising nanoparticle collector is a cationic polystyrene-co-poly(n-butylacrylate), which has not yet been used for separation of pyrite from lizardite slimes . Therefore, the objective of this study is to investigate whether this cationic polystyrene-co-poly(n-butylacrylate) can be selected as a nanoparticle collector to achieve effective separation between pyrite and lizardite slimes. For comparison, performance of potassium butyl xanthate collector was also tested in pyrite/lizardite slimes system. Microflotation experiments were conducted to evaluate the separation performance. The interaction mechanism between the collector and minerals surface was examined through adsorption, sedimentation, zeta potential test and DLVO calculations.

2. Materials and methods

2.1. The minerals and reagents

The pure pyrite and lizardite minerals used in this study were obtained from Jinchuan Group Co., LTD., China. Initially, the pyrite and lizardite specimens were manually crushed and ground. The size fraction of -10 μm lizardite and -37+74 μm pyrite was carefully collected for microflotation. The composition of MgO (40.26%), SiO_2 (42.37%), Fe (4.36%), Al2O3 (0.18%), CaO (0.17%) and others (12.66%) existed in the lizardite sample, the contents of Fe (46.06%), S (53.78%) and others (0.16%) in the pyrite sample. The X-ray diffraction (XRD) analysis of pyrite and lizardite is presented in Fig.1. The above analysis confirmed the absence of impurities in both pyrite and lizardite minerals, indicating that the samples met the experimental requirements in terms of purity.

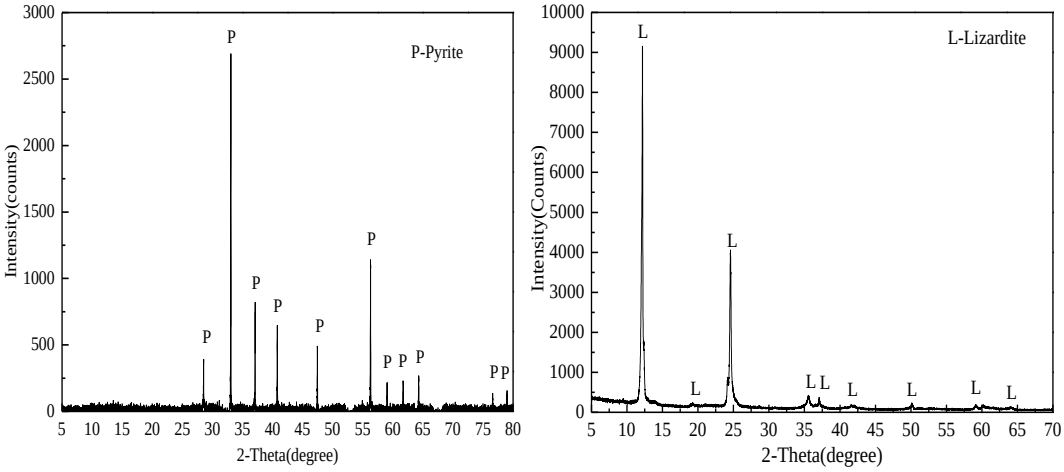

Fig. 1. The XRD patterns of lizardite and pyrite samples

In this study, the nanoparticle cationic polystyrene-co-poly(n-butylacrylate) (PS-PBNH) collector was synthesised using the following procedure. A mixture of phenylethylene and butyl acrylate with the mass ratio of 4:1 was used as the raw materials. The synthesis was conducted at a temperature of 70 ^{O}C for 24 hours using 2,2-azobis 2-methylpropionamidine dihydrochloride as initiator. Potassium butyl

xanthate collector (PBX) with approximately 89% purity was obtained from Chemistry and Chemical Engineering department of Central South University. Diluted NaOH and HCl were utilized as pH adjustor. The frother methyl isobutyl carbinol (MIBC) was analytical-grade. The distilled water was used throughout all the experiments, with conductivity value of 18.25MΩ/cm.

2.2. Micro-flotation tests

The microflotation tests were carried out using an XFGCII flotation machine, and the impeller speed was fixed at 1400 rpm. For each test, a mixture of 2 g pyrite or lizardite slimes (and the pyrite was treated though ultrasonic to remove the surface oxide film) and 40 mg distilled water was transferred into a 50 ml flotation cell. When required, 0.1g lizardite slimes was placed into the pyrite suspension, then adjusting the pulp pH and conditioning for 1 min. After that, the collector PBX (or PS-PBNH) and MIBC were orderly added in the suspension,and each addition was conditioned for 3 min and 1 min. The flotation time was conditioned for 4 min, then the floated and unfloated products were respectively collected, in the single mineral flotation, the mineral recovery was determined though the dry weight of the two products. In the mixture flotation, the floated product could used to represent the pyrite recovery because the extremely low floatability of lizardite slimes and the addition lizardite slimes were far lower than that of pyrite. In order to ensure the reliability of the flotation results, each flotation test was carried out three times, the final value was determined by the average of the tests and the error bar was exhibited though standard deviation.

2.3. Adsorption measurements

The adsorption of PS-PBNH on pyrite surface was performed by UV-2100 spectrophotometer. Before the measurements, the standard concentration curve of PS-PBNH was tested. For each test, a desired concentration of PS-PBNH was added into a mixture of 1 g pyrite (or 1 g lizardite) and 100 mL distilled water, and the pulp acid-base was fixed at pH 8.5. When needed, 0.5 g lizardite slimes was mixed with pyrite pulp. The minerals/distilled water mixture was conditioned for 10 min to ensure adsorption equilibrium. After that, the suspension was conditioned though centrifugal treatment. The adsorption amount was determined though the reduction between initial and residual dosages of PS-PBNH.

2.4. Sedimentation tests

Sedimentation tests were performed using a WZS-185A turbidity meter equipment. For each tests, 0.1 g of lizardite slimes (or 40 mg of PS-PBNH) and 100 mL solution were placed into a colorimetric tube. When required, 1 g of pyrite was added into the above solution. The suspension in colorimetric tube was inverted 30 times. After 3 min setting, the 25 mg/L of fixed height supernatant was collected and used for the sedimentation tests.

2.5. Zeta potential measurements

Zeta potential measurements were executed through a Malvern Instrument Nano-ZS90 analyzer. For the mineral samples, the mixure of 50 mg sample and 100 mL of 1×10^{-3} mol/L potassium chloride solution was magnetically stirred for 3 min at a specific pH value (pH range was from 4 to 12). After 10 min settling, the supernatant was collected for zeta potential measurements. For the nanoparticle collector, 400 mg/L of PS-PBNH was selected for zeta potential measurements. When required, the zeta potential of pyrite treated with collector was measured. To ensure the data accuracy, each sample was tested three times to obtain the average value as the final result. Additionally, the error bars were exhibited though the standard deviation calculations.

3. Results and discussion

3.1. Micro-flotation results

Fig. 2 illustrates the flotation performance of pyrite and lizardite slimes as a function of PS-PBNH collector dosage. As presented in Fig 2, the flotation recovery of lizardite was at around 18% without the addition of collector, and the lizardite recovery remained almost unchanged with the increase of PS-

PBNH collector dosage, suggesting that PS-PBNH does not have a significant collecting effect on lizardite. In contract, recovery of pyrite demonstrated improvement with increasing PS-PBNH collector dosage, up until a dosage of 400 mg/L PS-PBNH. Beyond this dosage, the recovery of pyrite remained unchanged. The maximum recovery of pyrite reaching to approximately 92%, was achieved when 400 mg/L PS-PBNH was used.

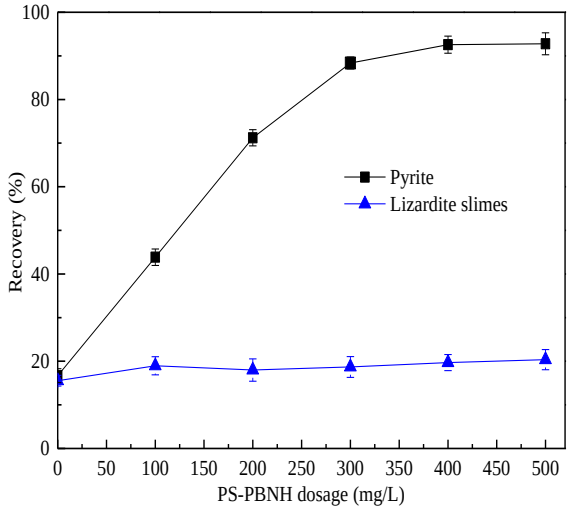

Fig. 2. Impacts of PS-PBNH dosage on the floatability of pyrite and lizardite (pH =8, MIBC = 1×10−4 M)

The floatability of pyrite, lizardite and their mixture under different pH condition is presented in Fig. 3. As shown, in the presence of PS-PBNH, the pyrite exhibited a good floatability in the pH range of 4-12. The flotation recovery of pyrite reached to ~90%, particularly at pH levels below than 9.0. However, as pH exceeded 9.0, the recovery of pyrite noticeably decreased. This phenomenon can be attributed to the presence of iron hydroxide at the pyrite surface as previously reported (Yuan et al., 2022). On the other hand, the flotation recovery of lizardite slim remained below 20% in the studied pH range. The significant difference in flotation behavior between pyrite and lizardite slimes illustrated that the potential for separating of pyrite from lizardite slimes in theory.

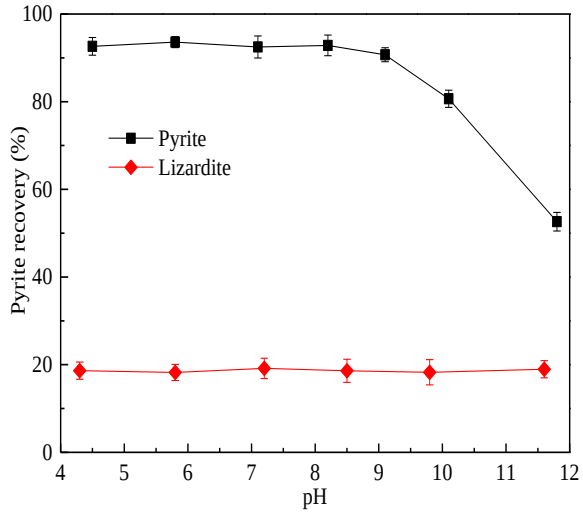

Fig. 3. Impacts of pH on the floatability of pyrite and lizardite under PS-PBNH (PS-PBNH=600 mg/L, MIBC = 1×10−4 M)

When lizardite slimes were mixed with pyrite, the pyrite floatability as a function of pH value was tested with the addition of PBX or/and PS-PBNH, and the results is presented in Fig. 4. As depicted, when the PBX was used as the collector, the flotation recovery of pyrite was decreased when the pH increased, and the recovery of pyrite was lower than 40% at the commonly performed pH rang of 8-9.

The results indicates that presence of lizardite slimes negatively affected the floatability of pyrite, similar to the previous work (Liu et al., 2018b). In contrast, when the nanoparticle PS-PBNH was used, the flotation recovery of pyrite remained consistently high. For instance, at pH 8.0, the recovery of pyrite was approximately 90%

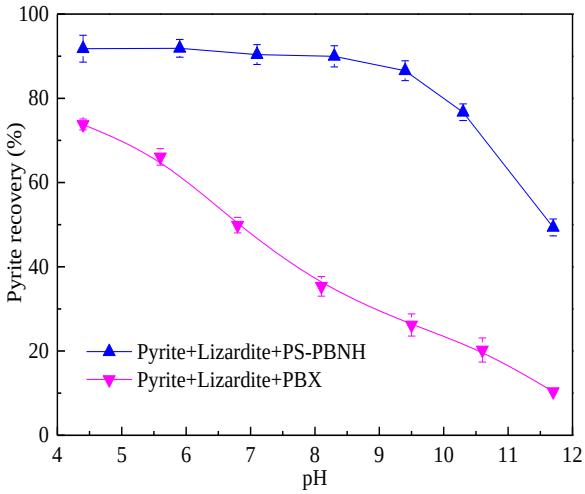

Fig. 4. The impact of lizardite slimes in pyrite flotation under different pH value (PS-PBNH=600 mg/L, PBX=50 mg/L, lizardite=50 g/L, MIBC = 1×10−4 M)

Fig. 5 illustrates the floatability of pyrite at pH~8 with varying collector dosages As shown in Fig 5, when the nanoparticle PS-PBNH collector was added in the mixture of pyrite and lizardite slimes, the pyrite recovery began to improve with increasing PS-PBNH collector. A maximum recovery of pyrite (around 90%) was obtained when the dosage of PS-PBNH exceeded 400 mg/L. In contrast, when PBX was added as collector to pyrite/Lizardite slimes system, the recovery of pyrite could not be restored even at high PBX dosages.

Considering the results from the Fig. 3, the flotation curve of pyrite indicated that the floatability of pyrite were restored in the presence of lizardite slimes when using PS-PBNH as the collector .

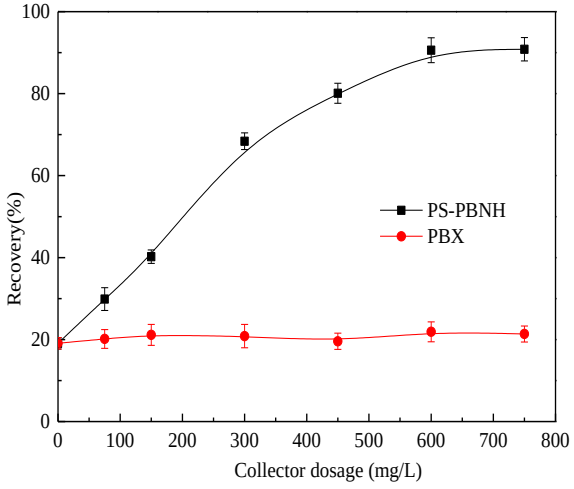

Fig. 5. Impacts of lizardite slimes in pyrite flotation under different collector dosage (pH=8.0, lizardite=50 g/L, MIBC = 1×10−4 M)

3.2. Adsorption results

To evaluate the adsorption performance of the collector on mineral surfaces. Fig. 6 shows the adsorption of nanoparticle PS-PBNH on the pyrite surface in the presence and absence of lizardite slimes.

As shown, the PS-PBNH could be adsorbed on the bare pyrite surface, and the adsorption amount increased with increasing the collector dosage. The effective adsorption of collector on pyrite surface corresponds to the observed floatability of pyrite in Fig. 2. In the case of individual lizardite, the addition of PS-PBNH resulted in negligible adsorption on the lizardite surface, illustrating the PS-PBNH was unable to adsorb onto the lizardite slimes surface. However, when the lizardite slimes were mixed with pyrite, the PS-PBNH collector adsorption was still occurred on pyrite surface but no adsorption of PS-PBNH on lizardite surface. Fig. 6 also shows that the adsorption amount of PS-PBNH on pyrite surface with presence of lizardite slims was slightly lower than that of on the bare pyrite surface, suggesting that lizardite slimes have a minor influence on the interaction between PS-PBNH collector and the pyrite surface.

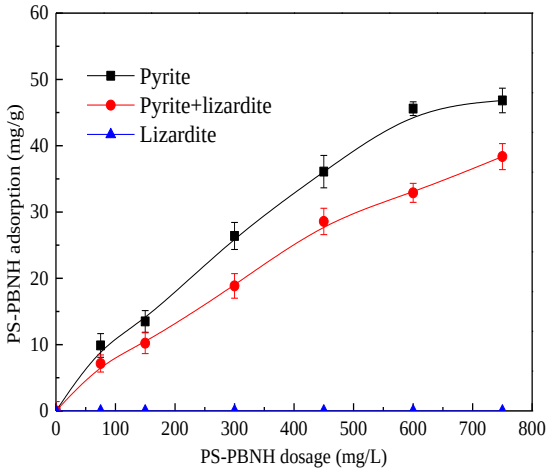

Fig. 6. The adsorption of PS-PBNH collector on minerals surface under different PS-PBNH dosage (pH=8.0, lizardite=50 g/L)

3.3 Turbidity results

To assess particle aggregation and dispersion, turbidity measurements were employed, where higher turbidity values indicate better dispersion between particles. Fig. 7 displays the turbidity values of individual samples and their mixtures at approximately pH 8.0. As shown, the turbidity value of pyrite, lizardite and nanoparticle PS-PBNH collector were 19 NTU, 812 NTU and 211 NTU, respectively. The turbidity of lizardite slimes was significantly higher than that of pyrite and PS-PBNH collector, indicateing that the turbidity of pyrite can be disregard in solution. Additionally, lizardite slimes and nanoparticle PS-PBNH collector readily despersed in solution.

When lizardite slimes were mixed with pyrite, the turbidity of the mixture of lizardite slimes and pyrite decreased to 593 NTU compared to the turbidity of the individual lizardite sample, suggesting that lizardite slimes coating occurred on pyrite particles surface. Regarding the mixture of pyrite and PS-PBNH, the turbidity of the mixture was 68 NTU which was lower than that of individual PS-PBNH, indicating that the PS-PBNH collector effectively interacted with pyrite surface, which agreed with the adsorption results. However, when the lizardite slimes was added in the pyrite/PS-PBNH mixture solution, the turbidity of pyrite/PS-PBNH/Lizardite mixture was significantly increased to 827 NTU, indicating that lizardite slimes could not interact with the nanoparticle PS-PBNH collector treated pyrite surface.

3.4. Electrokinetic behaviour results

The influence of pH on the zeta potential of pyrite, lizardite, the PS-PBNH collector, and PS-PBNH treated pyrite is plotted in Fig. 8. The zeta potential of pyrite and lizardite was decreased with increasing pH and their isoelectric points were observed at pH 11.1 and 3.7, respectively. This indicates that the surface charge of pyrite and lizardite had opposite polarity between pH 3.7 and pH 11.1. Hence, at the typical performed pH range of 8-9, the negatively charged pyrite surface could be coated by the positively charged lizardite slimes through the electrostatic attraction. As a result, the collector adsor-

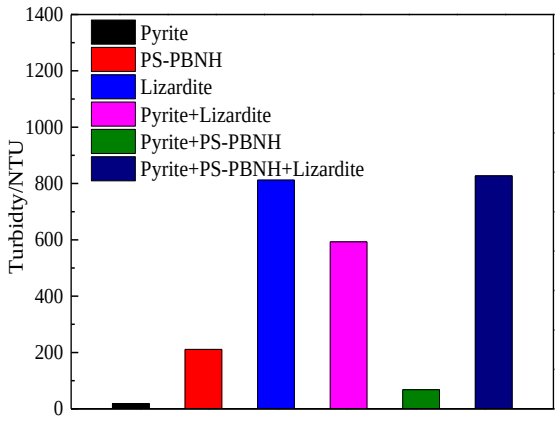

Fig. 7. The turbidity of single sample and their mixtures at pH 8.0 (Pyrite=10 g/L, Lizardite=1 g/L, PS-PBNH=600 mg/L)

ption on pyrite surface could be prevented when PBX was used as the collector in pyrite/lizardite slimes system (Abarca et al., 2015; Kusuma et al., 2014).

In the case of nanoparticle PS-PBNH collector, the zeta potential of PS-PBNH was remained positive across the pH range of pH 3.0-12.0, indicating a higher charge compared to lizardite. This can be attributed to the presence of cationic -NH_3^+ groups. The zeta potential of PS-PBNH treated pyrite surface was also positive, suggesting the adsorption of PS-PBNH on pyrite surface occurred. When the 600 mg/L PS-PBNH was added in the mixture of pyrite and lizrdite slimes, the interaction between pyrite and PS-PBNH was faster than that between pyrite and lizardite due to stronger electrostatic attraction between pyrite and PS-PBNH. As a result, lizardite did not coat the PS-PBNH treated pyrite surface due to electrostatic repulsion. Subsequently, the floatability of pyrite remained unaffected even when lizardite slimes were added in the pulp (see Fig. 5).

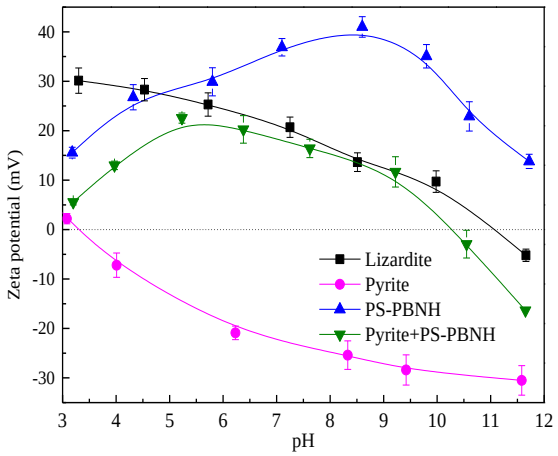

Fig. 8 The impact of pH on the zeta potential of different samples

3.6. DLVO theory calculation

To further investigate the interaction between pyrite and lizardite slimes, the classical DLVO theory was employed in the flotation system of pyrite/lizardite/PS-PBNH to calculated the particles interaction energy (Derjaguin and Landau, 1993; Gregory 1975). The total interaction energy V_T between particles can be described as the sum of the electrostatic energy V_E and the Van der Waals energy V_W (Ai et al., 2017; Yang et al., 2018).

$$V_T = V_E + V_W \quad (1)$$

$$V_W = -\frac{A}{6H}\frac{R_1 R_2}{R_1 + R_2} \tag{2}$$

$$A_{124} = (\sqrt{A_{11}} - \sqrt{A_{44}})(\sqrt{A_{22}} - \sqrt{A_{44}}) \tag{3}$$

$$V_E = \frac{\pi\varepsilon_0\varepsilon_r R_1 R_2}{(R_1 + R_2)}(\psi_1^2 + \psi_2^2)\cdot\left\{\frac{2\psi_1\psi_2}{(\psi_1^2 + \psi_2^2)}\cdot ln\left[\frac{1+exp(-\kappa H)}{1-exp(-\kappa H)}\right] + ln[1-exp(-2\kappa H)]\right\} \tag{4}$$

The Van der Waals interaction energy (V_W) between the particles can be described by Eq. 2, in this equation, A represents the Hamaker constant for the particles 1 and 2 in medium 3. For a vacuum system, A_{11} is for lizardite, A_{22} is for pyrite and A_{33} is for PS-PBNH, with the value of 9.7×10^{-20} J, 12.9×10^{-20} J and 5.84×10^{-20} J, respectively. A_{44} is Hamaker constant for the water medium with the value of 3.7×10^{-20} J (Bremmell et al., 2005; Feng et al., 2015; Vogiatzis and Theodorou, 2013). For example, the Hamaker constants A (A_{124}) of pyrite-lizardite-water medium can be determined using Eq. 3. In this equation R_1, R_2 and R_3 represent the radii of pyrite, PS-PBNH, and lizardite slimes, with the mean value of 46.2 μm, 0.2 μm and 7.3 μm respectively.

The electrostatic energy energy (V_E) between the different particles can be described by Eq. 4. In this equation, ε_0 represents the vacuum dielectric constant with the value of 8.854×10^{-12} $C^2/J\cdot m$, ε_r is the relative dielectric constant of the continuous phase with the value 78.5, κ is the reciprocal Debye length with the value of 0.104 nm^{-1}, and the ψ_1 and ψ_2 respectively represents the surface potentials of particle 1 and particle 2 respectively, commonly replaced by the zeta potential value.

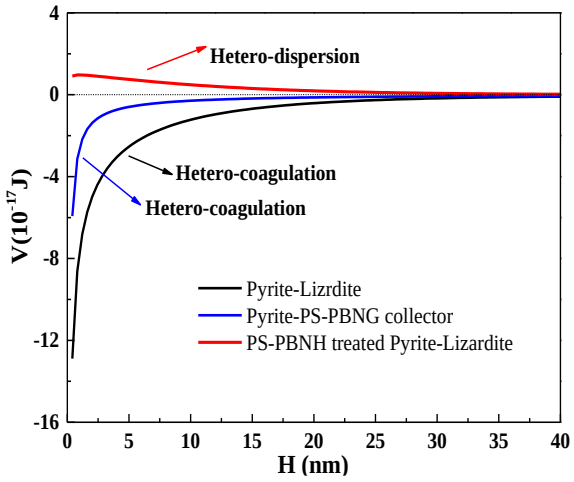

Fig. 9. The interaction energy between particles at pH 8.0

In Fig. 8, the zeta potential of pyrite, lizardite, PS-PBNH, and PS-PBNH treated pyrite were measured at the approximately pH 8.0, and found to be -25 mV, 12 mV, 38 mV and 16 mV , respectively. Using the obtained data in the Eqs. 1~4, the interaction curves were calculated and presented in Fig. 9. It can be observed that the total interaction energy of between pyrite and lizardite indicated an attraction, which illustrated the hetero-coagulation between lizardite slimes and pyrite.

Interestingly, the interaction energy between pyrite and PS-PBNH was also negative, suggesting that PS-PBNH collector could absorb on the pyrite surface. The absolute value the interaction energy between pyrite and PS-PBNH collector was lower than that between pyrite and lizardite due to the extremely low size of the PS-PBNH nanoparticle collector. However, the nanoparticle PS-PBNH readily interacted with pyrite surface due to its higher surface charge comparted to lizardite particles. As a results, when numerous PS-PBNH nanoparticles interacted with pyrite surface, thesurface charge of pyrite changed from negative to positive. The interaction energy of PS-PBNH treated pyrite with lizardite surface was positive, suggesting that lizaridite did not interacted with the PS-PBNH treated pyrite surface. Under these conditions, air bubbles could attached to the PS-PBNH treated pyrite surface, facilitating pyrite flotation in the pyrite/lizardite slimes system. The proposed interaction and flotation mechanism of pyrite/lizardite slimes with and without addition of PS-PBNH is schematized in Fig. 10

which further cleared why the pyrite floatability could be restored in this process. As shown in Fig.10, the lizardite slimes coating pyrite surface were unable to interacte with PBX/bubble due to the hydrophily of lizardite surface. However, when the nanoparticle PS-PBNH collector was used to as replacement for the PBX collector, the positive groups of the PS-PBNH collector could be interacted with pyrite surface. Consequently, the pyrite surface charge changed to positive, repelling the positively charged lizardite slimes. Additionally, the hydrophobic natural of nanoparticle allow it interact with the air bubble, leading the floatability of pyrite.

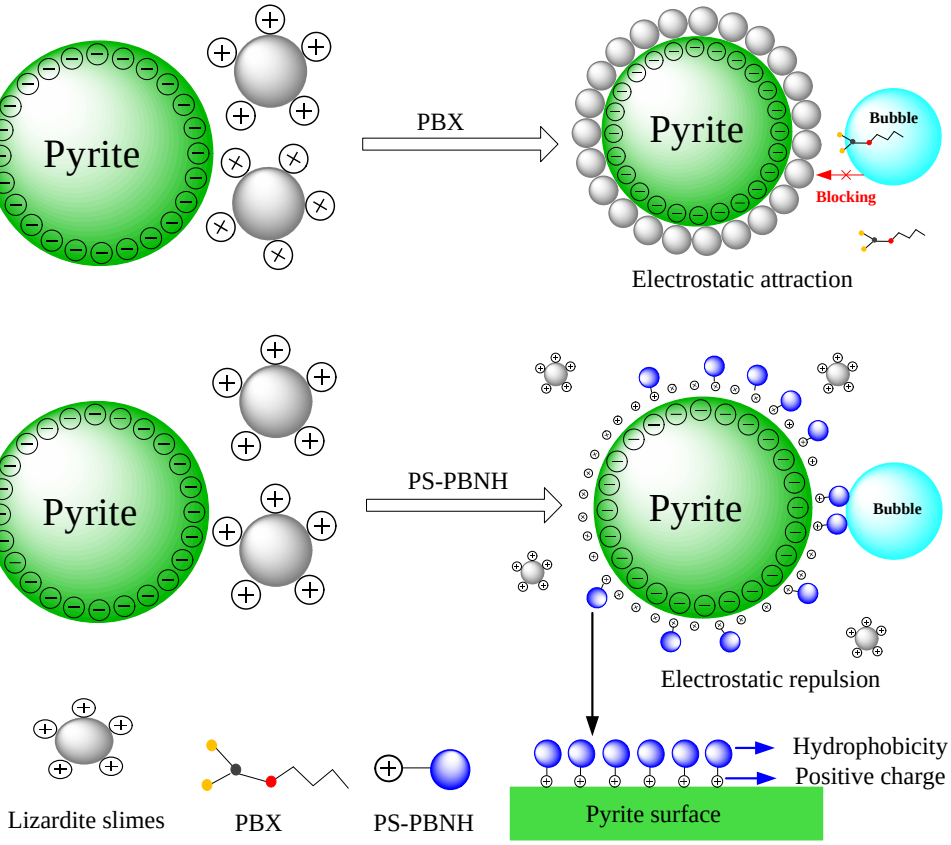

Fig. 10. The interaction model of pyrite/lizardite slimes mixture with PBX or PS-PBNH collector

4. Conclusions

The microflotation results demonstrate that the novel nanoparticle cationic PS-PBNH collector significantly decreased the negative impact of lizardite slimes in pyrite flotation. The turbidity measurements results revealed that lizardite slimes interacted with pyrite surface but did not interact with PS-PBNH treated pyrite surface. The results from zeta potential measurements implied that the PS-PBNH could be absorbed onto the surface of pyrite, leading to the a change in surface charge from negative to positive. Consequently, adsorption of the positively charged lizardite slimes could be provented from pyrite surface due to electrostatic repulsion between lizardite slimes and PS-PBNH treated pyrite. The results from DLVO calculations further supported these finding, confirming that the interaction energy between pyrite with lizardite slimes was negative, while that between PS-PBNH treated pyrite and lizardite slimes was positive. Based on these results, it can be conluded that the nanoparticle PS-PBNH collector can be used as an effective collector to significantly reduce the negative impact of lizardite slimes coating in the pyrite flotation.

Acknowledgments

The authors would like to acknowledge the support from the Natural Science Foundation of China (Nos. 52274269, 52004250) and the National Key Research and Development Program of China (No. 2022YFE0126800).

References

ABARCA C, YANG S, PELTON R. 2015. *Towards high throughput screening of nanoparticle flotation collectors.* J. Colloid Interface Sci. 460, 97-104.

ADEBAYO, G., ZHANABERGENOV, Z., ERNAZAROV, U., BADMUS, B., ANUSIONWU, B., 2014. *First principles study of electronic structure, structural and optical properties of $Mg_3Si_2O_5(OH)_4$.* Appl. Clay Sci. 93-94, 8-11.

AI, G., HUANG K., LIU C., YANG S., 2021. *Exploration of amino trimethylene phosphonic acid to eliminate the adverse effect of seawater in molybdenite flotation*. Int. J. Min. Sci. Technol. 31(6), 1129-1134.

BAILEY, S., 1988. *Polytypism of 1:1 layer silicates. Reviews in Mineralogy and Geochemistry*. 19(1), 9-27.

BREMMELL, K., FORNASIERO, D., RALSTON, J., 2005. *Pentlandite–lizardite interactions and implications for their separation by flotation*. Colloids Surf. A Physicochem. Eng. Asp. 252, 207-212.

DENG, J., YANG, S., ZHANG, W., LIU, C., LI, H., 2020. *The effect of lizardite on talc flotation using carboxymethyl cellulose as a depressant.* Physicochem. Probl. Miner. Process. 56(4),702–709

DERJAGUIN, B., LANDAU, L., 1993. *Theory of the stability of strongly charged lyophobic sols and of the adhesion of strongly charged particles in solutions of electrolytes*. Prog. Surf. Sci. 1993, 43: 30-59.

DONG, X., MARWAY, H., CRANSTON, E., 2016. Pelton RH. *Relating nanoparticle shape and adhesiveness to performance as flotation collectors*. Ind. Eng. Chem. Res. 55(36), 9633–9638.

EVANS, B., HATTORI, K., BARONNET, A., 2013. *Serpentinite: what, why, where?*. Elements, 9(2), 99-106.

FENG B, LU Y, LUO X, 2015. *The effect of quartz on the flotation of pyrite depressed by serpentine.* Journal of Materials Research and Technol. 4(1), 8-13.

FENG, B., PENG J., ZHANG, W., LUO, G., WANG, H., 2018. *Removal behavior of slime from pentlandite surfaces and its effect on flotation*, Miner. Eng. 125, 150-154.

FENG, B., LU, Y., FENG, Q., LI, H., 2012. *Solution chemistry of sodium silicate and implications for pyrite flotation.* Ind. Eng. Chem. Res. 51(37), 12089-12094.

FENG, B., LUO, X., 2013. *The solution chemistry of carbonate and implications for pyrite flotation,* Miner. Eng. 53, 181-183.

FROST, B., EVANS, K., SWAPP, S., BEARD, J., MOTHERSOLE, F., 2013. *The process of serpentinization in dunite from New Caledonia*. Lithos. 178, 24-39.

GREGORY J.,1975. Interaction of unequal double layers at constant charge. J. Colloid Interface Sci. 51 (1), 44-51.

KUSUMA, A., LIU, Q., ZENG, H., 2014. *Understanding interaction mechanisms between pentlandite and gangue minerals by zeta potential and surface force,* Miner. Eng. 2014, 69, 15-23.

LIU, C., AI, G., SONG, S., 2018a. *The effect of amino trimethylene phosphonic acid on the flotation separation of pentlandite from lizardite*. Powder Technol. 336, 527-532.

LIU, C., CHEN, Y., SONG, S., LI, H., 2018b. *The effect of aluminum ions on the flotation separation of pentlandite from lizardite.* Colloids Surf. A Physicochem. Eng. Asp. 555, 708-712.

LIU, C., ZHEN, Y., YANG, S., FU, W., CHEN, X., 2021. *Exploration of a novel depressant polyepoxysuccinic acid for the flotation separation of pentlandite from lizardite slimes*. Appl. Clay Sci. 202, 105939.

MAO, Y., XIA, W., PENG Y., XIE, G., 2022. *Dynamic pore wetting and its effects on porous particle flotation: A review.* Int. J. Min. Sci. Technol. 32(6), 1365-1378.

O'HANLEY D., 1996. *Serpentinites:Records of Tectonic and Petrological History*. New York: Oxford University Press.

SIROTA, V., SELEMENEV, V., KOVALEVA, M., PAVLENKO, I., MAMUNIN, K., DOKALOV, V., YAPRYNTSEV, M., 2018. *Preparation of crystalline $Mg(OH)_2$ nanopowder from serpentinite mineral.* Int. J. Min. Sci. Technol. 28(3), 499-503.

TANG, X., CHEN, Y., 2022. *A review of flotation and selective separation of pyrrhotite: A perspective from crystal structures*. Int. J. Min. Sci. Technol. 32(4), 847-863.

WICKS, F., WHITTAKER, E., 1975. *A reappraisal of the structures of the serpentine minerals.* The Canadian Mineralogist. 13(3), 227-243.

VOGIATZIS, G., THEODOROU, D., 2013. *Structure of polymer layers grafted to nanoparticles in silica-polystyrene nanocomposites*. Macromolecules 46, 4670-4683.

YANG, H., QIU, X., YAN, H., WU, H., YANG, L., LAI, R., QIU, T., 2022. *Investigating the selectivity of calcium hypochlorite for flotation separation of chalcopyrite and pyrite pre-adsorbed collector*. Physicochem. Probl. Miner. Process. 58(4), 150703.

YANG, S., XU, Y., LIU, C., AI, G., YU, H., 2020. *A novel method to achieve the flotation of pyrite from lizardite slime without collector or depressant*. Miner. Eng. 157(12), 106580.

YANG, S., PELTON, R., RAEGEN, A., MONTGOMERT, M., DALNOKI-VERESS, K., 2011. Nanoparticle flotation collectors: mechanisms behind a new technology. Langmuir: 27(17), 10438-10446.

YANG S, PELTON R., 2011. Nanoparticle flotation collectors II: *The role of nanoparticle hydrophobicity*. Langmuir, 27, 11409-11415.

YANG, S., PELTON, R., ABARCA, C., DAI, Z., MONTGOMERT, M., XU M, BOS, J., 2013. *Towards nanoparticle flotation collectors for pentlandite separation.* Int. J. Miner. Process. 2013, 123, 137-144.

YANG, S., PELTON, R., MONTGOMERY, M., CUI Y., 2012. *Nanoparticle flotation collectors iii: the role of nanoparticle diameter*. Acs Applied Materials & Interfaces, 2012, 4(9), 4882-4890.

YANG, S., XIE, B., LU, Y., LI, C., 2018. *Role of magnesium-bearing silicates in the flotation of pyrite in the presence of serpentine slimes*. Powder Technol. 332, 1-7.

YUAN, J., DING, Z., BI, Y., LI, J., WEN, S., BAI, S., 2022. *An innovative flotation technology for the lime-depressed pyrite recovery from copper sulfide ore via acid mine drainage (AMD) activation*. Physicochem. Probl. Miner. Process. 58(6), 152609.

YU, X., HU, L., LIU, C., WANG, L., LI, H., XUE, L., 2019. *The effect of 2-phosphonobutane-1,2,4-tricarboxylic acid on the flotation separation of pyrite from lizardite.* Colloids Surf. A Physicochem. Eng. Asp. 2019, 570, :317-321.

ZHANG, C., LIU, C., FENG, Q., CHEN, Y., 2017. *Utilization of N-carboxymethyl chitosan as selective depressants for serpentine on the flotation of pyrite.* Int. J. Miner. Process. 163, 45-47.